Available online at www.sciencedirect.com

ScienceDirect

Ceramics International 40 (2014) 3079–3087

CERAMICS INTERNATIONAL

www.elsevier.com/locate/ceramint

Preparation of a hemiporous hydroxyapatite scaffold and evaluation as a cell-mediated bone substitute

Jeong Joon Yoo[a], Hee Joong Kim[a,b], Sang-Min Seo[c], Kyung-Sik Oh[c,*]

[a]Department of Orthopedic Surgery, Seoul National University College of Medicine, 101 Daehak-ro, Jongno-gu, Seoul 110-744, South Korea
[b]Medical Research Center, Seoul National University, 101 Daehak-ro, Jongno-gu, Seoul 110-744, South Korea
[c]School of Advanced Materials Engineering, The Center of Biomedical Materials and Biotechnology, Andong National University, South Korea

Received 24 July 2013; received in revised form 29 September 2013; accepted 29 September 2013
Available online 8 October 2013

Abstract

A hemiporous hydroxyapatite (HAp) scaffold was prepared to support the tissue engineered approach to the restoration of damaged bone. The scaffold comprised a porous cell-seeded part and a non-porous load bearing part. A wet processing technique of HAp suspensions was used to shape the hemiporous body. The structure of the porous part was tailored using a stack of heat treated porogen placed on the plaster. The prepared specimen had approximately 30 layers of connected pores, which could accommodate sufficient human bone marrow stromal cells (hBMSCs). The result of an *in vitro* test showed that hBMSCs successfully proliferated and produced extracellular matrices even at the pore in the deep portion of the scaffolds. The *in vivo* test in the distal femur of a rabbit showed the formation of new fibrous tissue and tubular vessels with red blood cells in the hBMSCs-seeded scaffold from the pores at the deepest portion as well as from the pore at the periphery of the scaffold. The result was in distinct contrast with the scaffold without cell loading. The preloading of cell was thus very effective in the migration of cells in spite of the unconfirmed connectivity among pores. The present casting approach had the merits of simplicity and versatility in tailoring the scaffold structure without an elaborate device.
© 2013 Elsevier Ltd and Techna Group S.r.l. All rights reserved.

Keywords: Hydroxyapatite; Bone marrow stromal cell; Scaffold; Preloading; *In vivo*

1. Introduction

Many challenges are involved in the treatment of bone loss conditions such as non-union, periprosthetic bone defect, and posttraumatic or postsurgical bone loss. In many cases, adjunctive measures such as bone-grafting or bone substitute implantation are required to stimulate bone-healing and fill bone defects. Autologous or allogenic bone graft, demineralized bone matrix, and synthetic bone substitute are options for these conditions. However, their shortcomings include donor-site morbidity, limited volume available, immunogenicity, disease transmission risk, and high costs [1,2]. Especially, synthetic bone substitutes do not have internal osteoinductive acting cells, rendering their biological functions limited [1,2].

Cell-seeded bone substitute is a novel tissue engineered approach used to render osteoinductive synthetic bone substitute. Before implantation, cells are infiltrated into the substitute and are then cultured. Thus, the scaffold inevitably requires a highly open structure for the accommodation of sufficient cells. To ensure the connected structure of the pores, the porosity of the substitute needs to be fairly high. However, the increased porosity is critically disadvantageous to the load bearing capability, *i.e.* strength. The decrease in strength limits an applicability of the scaffold as well as the ease of handling during cellular introduction and implantation. It should be noted that the strength of natural bone relies on the dense cortical bone. Therefore, inspired from the natural structure of bone, the strengthened scaffold can be designed by providing a dense support for load bearing.

In this context, the Hydroxyapatite (HAp) specimen composed of porous body and dense support is prepared and evaluated. The specimen was termed as hemiporous scaffold, since half of the scaffold was porous. HAp, the mineral part of natural bones, is capable of guiding bone formation [3]. In a previous report [4], even chemical bonding with natural bone was claimed due to the

*Corresponding author. Tel.: +82 54 820 5783; fax: +82 54 820 6211.
E-mail address: ksoh@anu.ac.kr (K.-S. Oh).

0272-8842/$ - see front matter © 2013 Elsevier Ltd and Techna Group S.r.l. All rights reserved.
http://dx.doi.org/10.1016/j.ceramint.2013.09.138

chemical similarity. HAp has, therefore, been widely used as a synthetic bone substitute [5–7].

Human bone marrow stromal cells (hBMSCs) are potentially good candidates for the cell-mediated tissue engineered approach to address a variety of unsolved medical situations, particularly in the musculoskeletal area, owing to their relatively good availability and biological characteristics [8–10]. hBMSCs have the capacity of self-renewal and can differentiate into several types of mesenchymal cells, including osteoblasts, chondrocytes, and adipocytes [8–10].

In this study, a hemiporous HAp scaffold was evaluated both *in vitro* and *in vivo* with hBMSCs. The hBMSCs were cultured in the scaffold for 14 days before implantation to achieve migration and successive proliferation. In addition, we evaluated the tissue regeneration ability of hBMSCs-seeded hemiporous HAp in the distal femoral bone defects of rabbits. The results were compared with the same scaffold without cell loading. We hypothesized that the cellular responses of hBMSCs in the porous region of a hemiporous HAp scaffold might be acceptable *in vitro*. We also postulated that the hBMSC-loaded hemiporous HAp scaffold would enhance bone formation at an orthopedic surgical site *in vivo*.

2. Materials and methods

2.1. HAp suspension preparation

An aqueous processing route was selected for the preparation of the porous scaffold. HAp powder (Sigma-Aldrich, St. Louis, MO, USA; 34.0–40.0% Ca) was attrition milled (KMC-1B, KMC, Seoul, Korea) using 5 mm diameter zirconia balls as media. Darvan C (Vanderbilt Co. Norwalk. CT, USA) was introduced as a dispersant. The suspension was prepared through the measurement of the viscosity as a function of various parameters such as pH and solid loading. The pH of the suspension was controlled by introducing NH_4OH. A concentrated HAp suspension with minimized viscosity was prepared through the careful control of parameters including the amount of dispersant, pH, solid loading and milling time as reported previously [11]. The particle size in the suspension was estimated to be 0.3 μm according to the analysis based on laser diffraction (Mastersizer 2000, Malvern, England).

2.2. HAp substitute with porous layer on the surface

Porogen Sephadex G-50 polymer beads (Sigma-Aldrich, St. Louis, MO. USA, Fig. 1a) with a diameter of 300–350 μm provided the template to form a porous structure. Sephadex is a cross-linked dextran gel synthetically derived from the polysaccharide, dextran. Complete removal of porogens could be verified by burning out at 400 °C. The stack of polymer beads with uniform thickness was prepared by placing them between two glass plates. The stack was heat treated at 230 °C for 2 h to partially bond the porogens (Fig. 1b). The heat treated stack was placed on a plaster block with a cylindrical rubber mold in a similar way to that reported [12] previously. The green body was formed by pouring the HAp suspension into the cylindrical mold. With the drying of the slip cast specimen, shrinkage of the green body was observed. The specimen was thus dried at room temperature to facilitate slow drying. After drying, the specimen was heated to 400 °C at a rate of 2 °C/min to burn out the porogens and was subsequently consolidated by sintering at 1200 °C for 2 h.

2.3. Structural characterization

The specimen was impregnated in the diluted resin to evaluate the connectivity of the pores. As soon as the resin solidified, the specimens were vertically bisected with a diamond saw for microstructural analysis. The exposed surface was sequentially polished with SiC abrasive paper to reveal the pores filled with resin. Scanning electron microscopy was performed using a JSM-6300 apparatus (Jeol, Tokyo, Japan) at an accelerating voltage of 20 kV. Connectivity was estimated by measuring the volume fraction of resin-filled pores among the total volume of pores from the polished cross section.

2.4. Measurement of load bearing capability

The load bearing capability of the specimen was measured using a model 810 universal testing machine (MTS810, Eden Prairie, MN, USA) at a crosshead speed of 0.5 mm/min. The load for fracture was tested either by axial or diametral compression.

2.5. Isolation and seeding of hBMSCs

After institutional review board approval (IRB H-1010-074-337), fresh bone marrow was aspirated from the iliac crests of patients undergoing total hip arthroplasty. A 14-gauge needle was inserted into the iliac tuberosity adjacent to the anterior superior iliac spine, and 6–7 mL of marrow was aspirated. Two more aspirates were obtained through the same cortical hole, but at a different depth. Twenty milliliters of bone marrow aspirates were collected from each patient into a syringe containing 6000 units of heparin. hBMSCs were isolated from the marrow aspirates using a modified version of the previously detailed procedures [10,13]. The aspirates were washed with Dulbecco's phosphate-buffered saline (DPBS; GibcoBRL®, Gaithersburg, MD, USA), and the cells were recovered following 10 min of centrifugation at 900*g*; this process was repeated once. The washed cells were subsequently re-suspended in DPBS to a final density of 4×10^7 cells/mL. A 5 mL aliquot was layered over 1.073 g/mL of Percoll solution (Pharmacia®, Piscataway, NJ, USA) in a 50 mL conical tube and centrifuged for 30 min at 1100*g*. Nucleated cells collected at the interface were recovered and counted using a hemacytometer. The collected nucleated cells were then re-suspended in a human mesenchymal stem cell (MSC) medium and plated in 150 mm diameter Petri dishes at a density of 2×10^6 cells/cm^2 in 30 mL of medium. The human MSC medium consisted of Dulbecco's Modified Eagles Medium-Low Glucose (DMEM-LG; GibcoBRL®) supplemented with 10% fetal bovine serum (FBS; GibcoBRL®)

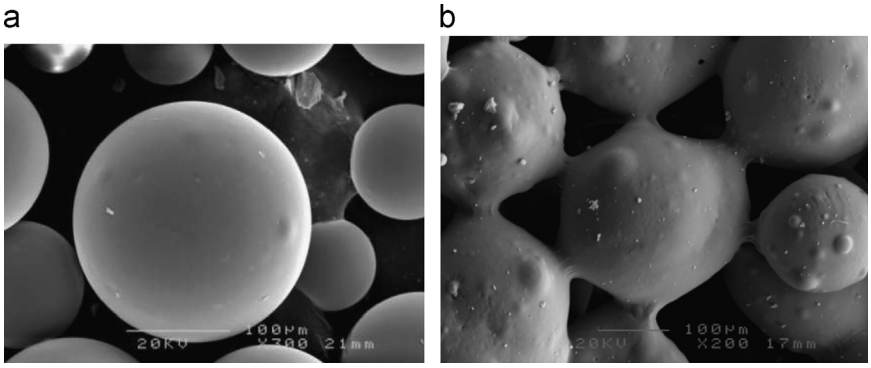

Fig. 1. Porogens used for the experiment (a) as received and (b) after heat treatment at 230 °C for 2 h.

and 1% Anti–Anti (Antibiotic–Antimycotic, penicillin G sodium 100 U/mL, streptomycin 100 μg/mL, and amphotericin B 0.025 μg/mL; GibcoBRL®). The hBMSC cultures were maintained in 5% CO_2 at 37 °C, and the medium was replaced at 24 and 72 h and every 3–4 days thereafter.

At 80–90% confluency after the first passage, the hBMSCs (P1) were harvested, mixed, and seeded into the hydrated HAp substitute. The cylindrical hemiporous HAp scaffolds with measurements of 8 mm diameter and 6 mm height with a 3 mm porous portion were prepared for *in vitro* studies. Briefly, the 20 μL aliquots of the hBMSC suspension containing 2×10^5 cells were dropped onto the porous surface of scaffolds using a micro-pipette, and were allowed to infiltrate into the scaffolds on sterilized Kimwipes. The cells of the cell-seeded specimens were then allowed to attach to the scaffold for 4 h at 37 °C in a humidified 5% CO_2 incubator. After adding osteogenic culture medium, the specimens were incubated *in vitro* for 14 days at 37 °C in 5% CO_2. The osteogenic medium consisted of DMEM-LG supplemented with 10% FBS, 200 mM of L-glutamine (Sigma-Aldrich®), 0.1 μM of dexamethasone (Sigma-Aldrich®), 50 μg/mL of ascorbic acid-2-phosphate (Sigma-Aldrich®), 10 mM of β-glycerophosphate (Sigma-Aldrich®), and 1% Anti–Anti [13,14].

2.6. Attachment, proliferation, and alkaline phosphatase activities of hBMSCs

For hBMSC attachment and proliferation assays, the number of cells in the scaffold was counted using a CCK-8 cell counting kit (Dojindo, Tokyo, Japan) at 24 h and 7 days after seeding, as follows. The scaffolds were washed with DPBS after removal of the medium, and protected from light. The CCK-8 solution was added and the mixtures were incubated for 3 h at 37 °C, so that the colored formazan product would appear by dehydrogenases of the hBMSCs. Subsequently, the absorbance at 450 nm was measured using a VERSAmax tunable microplate reader (Molecular Devices, Sunnyvale, CA, USA). The cell counts were calculated from the absorbance, using a standard curve.

To assess the osteogenic differentiation of hBMSCs, the alkaline phosphatase (ALP) activity of the cultured hBMSCs in the scaffold was determined using an ALP diagnostic kit (Sigma-Aldrich®) at 7 and 14 days. The cell lysate specimens were obtained by treating cultures with 0.1% Triton X in water. Ten microliters of each specimen was introduced onto 24-well plates. Fifty microliters of ALP buffer (Sigma-Aldrich®) were added to each well, and the plates were shaken for 30 min at room temperature. Subsequently, 50 μL of 0.05 N NaOH was added, after which the plate was shaken for 5 min. Finally the absorbance of the reaction product, p-nitrophenol, was measured at 405 nm on a VERSAmax tunable microplate reader. ALP activity was calculated from the absorbance. The reference sample was prepared with p-nitrophenol standard (Sigma-Aldrich®). The activities were recorded in terms of μmol p-nitrophenol/min/mg of protein per well. The measured ALP activities were normalized *versus* the total protein content, which was determined with a protein assay kit II (BIO-RAD Laboratories, Hercules, *CA*, USA). The ALP activities of the cells cultured on the tissue culture plate (TCP) were measured as a control.

2.7. Field emission scanning electron microscopic (FE-SEM) observation

The scaffolds were examined with the FE-SEM 14 days after the osteogenic differentiation culture. The microstructural morphology of the scaffold and the seeded hBMSCs was evaluated. The specimens were obtained after removal of the medium, and washed three times with DPBS. They were fixed for 2 h with 1000 μL of 2% glutaraldehyde (Sigma-Aldrich®) at 4 °C. They were then washed with DPBS and dehydrated by soaking serially in increasing concentrations of ethyl alcohol (70–100%), followed by drying *in vacuo*. The specimens were cut into two pieces with a chisel and covered with gold–palladium alloy on an aluminum stub and examined via FE-SEM using a S-4700 apparatus (Hitachi, Tokyo, Japan) under 15 kV.

2.8. In vivo studies

The Institutional Animal Care and Use Committee of our hospital approved all animal procedures. The cylindrical hemiporous HAp scaffolds, with measurements of 6 mm diameter and 8 mm height with a 4 mm porous part, were

prepared for *in vivo* studies. Animal experiments were divided into two groups (hBMSCs-seeded hemiporous HAp scaffold and the scaffold without cell loading, n=5 for each group) and were conducted using rabbits. After 14 days of osteogenic differentiation culture, the cell-seeded scaffolds were implanted into the distal femoral bone defects of rabbits.

The rabbits were anesthetized by the intramuscular injection of ketamine sodium (10 mg/kg) and xylazine hydrochloride (20 mg/kg). A 2-cm longitudinal skin incision was made on the medial aspect of each leg proximal to the knee joint line. The periosteum was retracted and the medial aspect of the distal femur was exposed. An 8-mm deep hole was transversely made through the femoral metaphysio-diaphyseal junction 10 mm apart from the articular surface using a 6-mm drill bit. After gauze packing for 10 min to control the bleeding and washing with a sterile physiological saline solution, a specimen was inserted into the hole facing the porous part inside, and the non-porous part was press-fitted in the cortical bone. The specimens, in which the cells were not seeded, were implanted as a control. After surgery, no specific joint protection apparatus was used. The rabbits were allowed to walk with full weightbearing as tolerated. At 8 weeks after implantation, the specimens were harvested from rabbits.

The specimens were fixed with 10% neutral formalin, and embedded in Technovit 7200 VLC resin (Heraeus KULZER, Germany). Undecalcified ground sections (50 μm thick) parallel to the longitudinal axis of the scaffold were prepared from the mid-portion of the specimen using a 300 CP diamond saw cutting system (EXAKT Technologies, Inc, Germany) according to a previously detailed method [15] and stained with hematoxylin and eosin (HE).

2.9. Statistical analysis

The ALP activities of the hBMSCs cultured in the scaffold were compared with those of the cells cultured on the tissue culture plate (TCP) using a Mann–Whitney test. Examples of Mann–Whitney test with detailed procedure can be found in the report [16,17]. Differences were considered significant at $p < 0.05$.

3. Results

3.1. Preparation of the specimen and estimation of the connectivity

The HAp suspension used for the preparation of the specimens had a solid loading of 12.5 vol% with a viscosity of less than 0.01 Pa s as a result of the optimizations among parameters including the amount of dispersant, pH, and milling time [11]. The porogen stack (Fig. 2) heat-treated between the pair of glass plates had a thickness of 3.6 mm. Heat treatment of the stack of porogen at 230 °C for 2 h successfully joined the porogens by forming the necks as shown in Fig. 1b. The HAp suspension poured over the porogen stack successfully infiltrated and reached the plaster. As soon as the water was absorbed by the plaster, the HAp particles settled over the plaster and filled the space among the porogens. The HAp particles settling above the porogen stack subsequently built up the substrate of the specimen.

Fig. 2. Stack of porogens heat treated between the pair of glasses at 230 °C for 2 h.

Drying at room temperature for 7 days and subsequent heat treatment of the specimen to 400 °C decomposed the porogens and left the porous structure within the HAp specimen. Firing at 1200 °C for 2 h shrank the diameter of the specimen by 18%. Fig. 3a shows the specimen after consolidation. As shown in the cross section in Fig. 3b, the specimen prepared for the *in vitro* test had a diameter of 8 mm and a height of 6 mm with a 3 mm of porous portion. The average size of the pores was estimated to be 310 μm from microscopic observation in Fig. 3c, where the connection among the pores can also be verified. Observation under high magnification (Fig. 3d) showed that the substrate was not completely dense. According to the image analysis on the polished section, there was 3 vol% of isolated submicron pores, which is the result of incomplete densification.

Fig. 4 shows the cross section of the prepared hemiporous HAp scaffold impregnated with diluted resin. The resin infiltrated the open pores in the scaffold and brought about a setting reaction. Thus the external connection could be verified for an every single pore. Fig. 4 shows that several pores marked with circle remain unfilled. The infiltration of resin, therefore, allowed the estimation of the number fraction of externally connected pores among the pores greater than 200 μm. To evaluate the total volume of open pores of all sizes, Archimedes immersion is a well established approach. As the external connection is concern for the pores greater than 200 μm in this work, resin infiltration was used instead of Archimedes immersion. After all, at least 88% of the pores were externally connected according to the image analysis of Fig. 4.

3.2. Load bearing of the specimen

Fig. 5 shows the changes of stresses from a hemiporous scaffold in axial and diametral compressive strain. During the axial compression in Fig. 5a, two peaks of stress of fracture

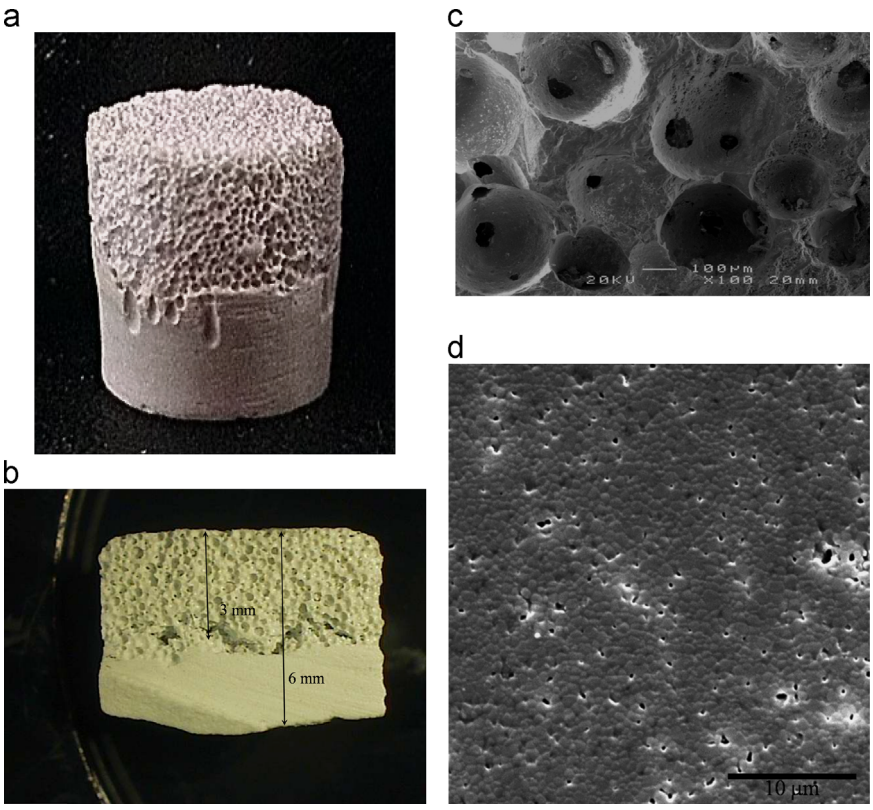

Fig. 3. Hemiporous HAp scaffold (a) overview, (b) cross section, (c) porous part, and (d) dense part.

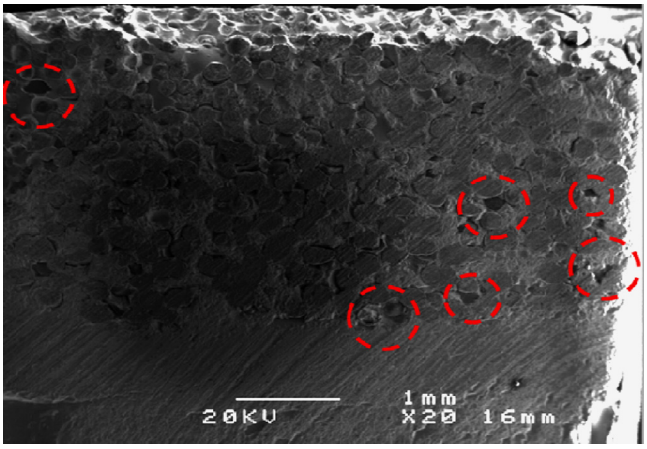

Fig. 4. Cross section of the prepared hemiporous HAp scaffold impregnated with setting resin. Circles denote pores which failed to be filled with resins.

appeared. The first peak was due to the fracture of the porous part at the strain of ~6% mm and the other peak was due to the dense part at strain of 25% mm. The peak due to the fracture of the dense part was much greater as 40.4 MPa compared with the other peak (14.7 MPa). In contrast, only one strong peak load of 6.4 MPa was recorded at very small displacement of 1.96% in diameteral compression (Fig. 5b). The compressive strength could be estimated by dividing the fracture load by the cross section for 5 specimens. As a result of the axial compression, the averages of strengths were 9.1 ± 3.2 MPa and 32.1 ± 9.0 MPa for the porous part and the dense part, respectively. The diameteral peak load (P) in Fig. 5b could be used to calculate tensile strength (σ_t) using Eq. (1) [18] for a specimen with a diameter D. Thickness (t) was taken from the height of the dense part. The tensile strength was estimated to be 10.1 ± 3.9 MPa.

$$\sigma_t = \frac{2P}{\pi D t} \tag{1}$$

The hemiporous specimen prepared in this work has a suitable shape for diametral compression, which is also known as the Brazilian test [18] as shown in the inset of Fig. 5c. During the diameteral compression, the horizontal stress σ_x is tensile with a constant value of over about three-quarters of the diameter, though it becomes compressive when approaching the contact points. In contrast, the vertical stress σ_y is compressive on the entire diameter, increasing from the center [18].

As a fracture results from a tensile stress, a crack thus propagates normal to the direction of a tensile stress. Thus a specimen should theoretically be vertically bisected by the diametral compression. The tensile fracture test can alternatively be carried out by direct tension, indirect tension, or 4 point bending. The merits of the diameteral compression compared with other methods include the simplicity of the preparation of the specimen and the relative insensitivity of the state of specimen surface. However, care should be taken in the accurate evaluation of tensile strength by the diametral compression.

The exactly bisected fracture in diameteral compression proves the failure at the plane of maximum stress. Unlike the

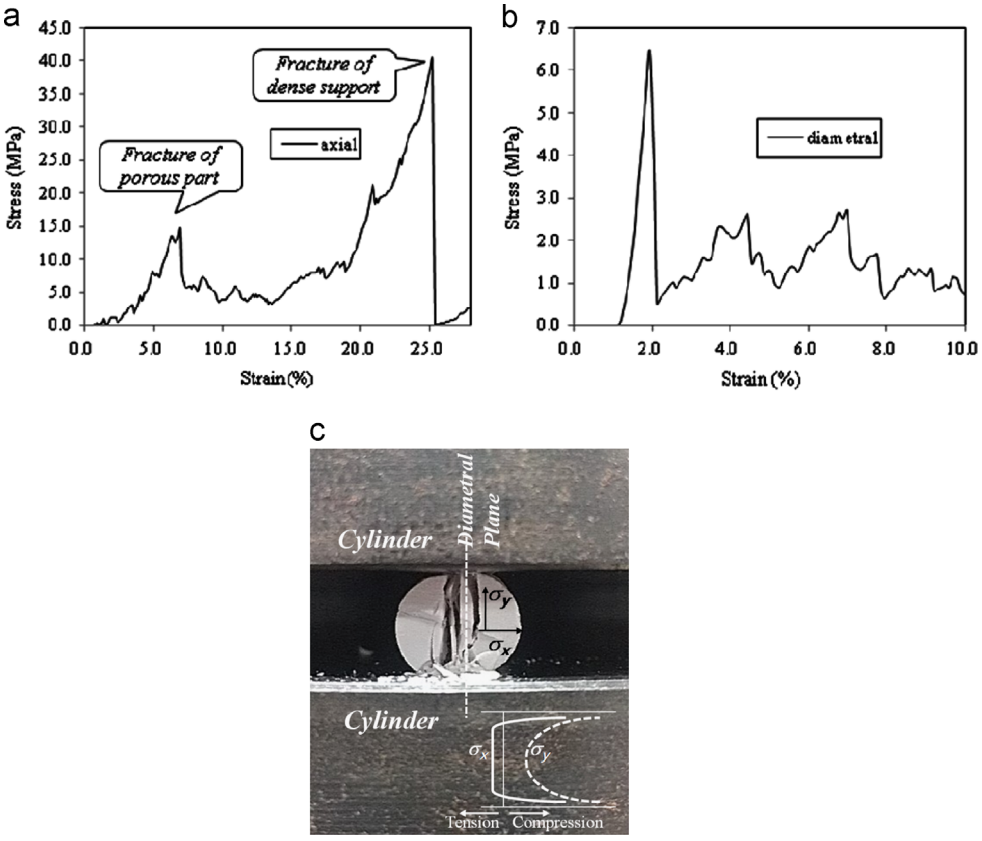

Fig. 5. Change of the stress as a function of the strain during the (a) axial and (b) diametral compression. (c) Specimen fractured as a result of diametral compression.

direct tension test, the stress distribution is not homogeneous in the diametral compression. As the tensile strength is sensitive to the existence of the pores, the fracture can initiate at the point distant from the center line. The tensile fracture propagates catastrophically from the pore, so the fracture load during diametral compression may be recorded at a reduced value compared with that at the center line. The results in Fig. 5 shows that the porous part has been effectively protected by the dense substrate and has obviously improved the ease of handling for the various cellular infiltration and implantation procedures in this work.

3.3. ALP activities and morphology of hBMSC

The seeding efficacy of hBMSCs was 94.6% at 24 h and the cell number of hBMSCs increased from 189 ± 6 to 286 ± 7 (thousand) on day 7 in the HAp scaffolds. The average fold-increase of the cell number was 1.5 at 7 days compared to 24 h of culture (Fig. 6a). ALP activities were lower on day 7, but reached a similar level in the HAp scaffolds on day 14 as compared to those observed on TCPs (Fig. 6b). FE-SEM demonstrated that hBMSCs proliferated and produced extracellular matrices covering the surface of the scaffolds both in the central and in the deep pores at 14 days of *in vitro* culture. Even in the deepest pore, hBMSCs formed a layer that completely covered the pore surfaces (Fig. 7).

3.4. Histological analysis

Histological evaluation demonstrated the presence of a newly formed bone tissue in the hBMSCs-seeded scaffold throughout the pores from the surface (Fig. 8a) to the deepest portion (Fig. 8c) after the 8-week *in vivo* period in the distal femur of rabbits. Tubular newly formed vessels, which contained red blood cells and which interconnected the pores, were also observed in both the surface and the deep portions. These findings showed that the pores were highly interconnected and the environment was optimal for the cellular migration, proliferation and differentiation, even in the deep pore region in hBMSC-seeded scaffolds. In contrast to these findings, even though sparse new bone tissue was observed in the pores of the surface (Fig. 8b), there was no evidence of newly formed tissue or vessels in the deep portion (Fig. 8d) of the scaffold without cell loading.

4. Discussion

The pore interconnectivity in the prepared porous body critically influences the success of nutrient supply [19], circulation of extracellular material [20], contact between adjacent cells [21], promotion of blood vessel formation [22], and bone tissue in-growth [23]. It is preferred that the macropores in the porous body are larger than 100 μm to enable the invasion of cells. Moreover, the interconnecting

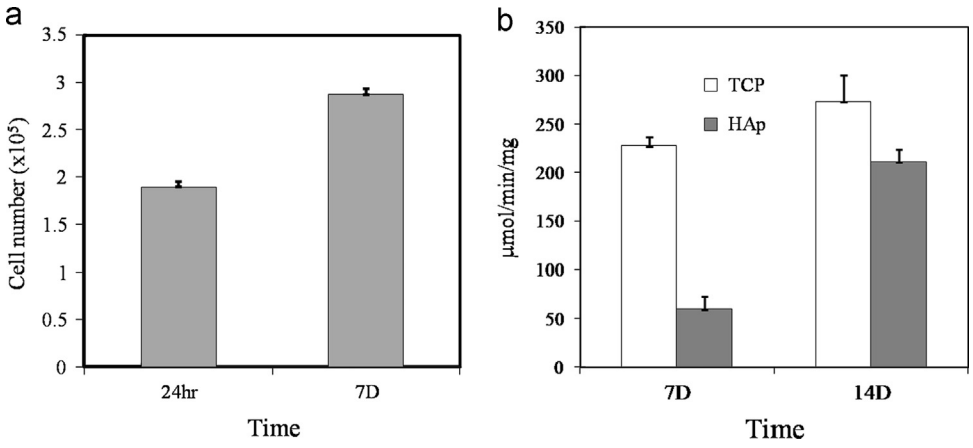

Fig. 6. (a) Attachment and proliferation of hBMSCs in hemiporous HAp scaffold during osteogenic differentiation. (b) ALP activity of hBMSCs in hemiporous HAp scaffold. The abbreviation-TCP denotes tissue culture plate.

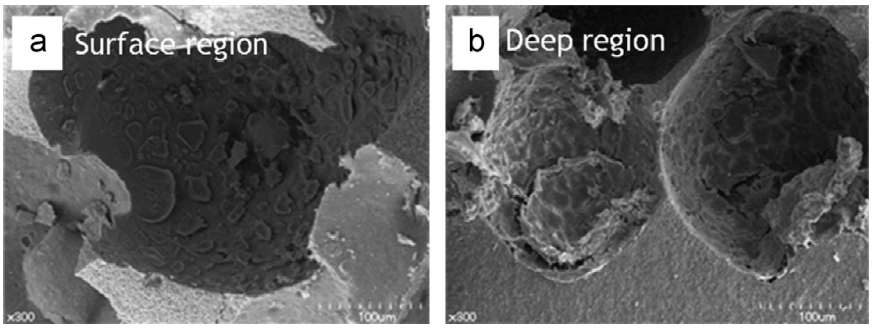

Fig. 7. FE-SEM examination of hBMSCs-seeded hemiporous HAp scaffold on day 14 after osteogenic culture (original magnification of × 300). (a) and (b) are photomicrographs taken from the surface and deepest pore, respectively.

necks of macropores should be of adequate size to transport osteogenic cells and nutriments. Interconnection pathways larger than 50 μm are necessary for osteogenesis [24].

The term, '(inter)connectivity' may mean the degree of the connection of pores. It should be noted that the meaning of connectivity depends on the researcher. Lemon [25] defined the connectivity as the volume fraction of connected pores. In contrast, Andersson [26] understood connectivity as the number of connected pores per single pore. In an ideal face-centered cubic arrangement of pores, there are twelve neighboring pores per a single pore. The connectivity is 12, if the pore is connected with all the neighboring pores. A pore connected with only one neighboring pore is regarded as a connected pore by Lemon's definition, but it has quite low connectivity according to Andersson's view.

If the arrangement of pores is not ideal, the determination of the average coordination number requires a structural investigation for every single pore. SEM has been widely used to investigate pore architecture and several approaches have been undertaken to determine connectivity qualitatively [20,27,28]. SEM only allows two-dimensional measurements in a limited field of view [22,29] and is therefore inadequate to obtain Andersson's connectivity. Three-dimensional structural information obtained by X-ray micro-CT can contribute in the estimation of Andersson's connectivity [30,31].

SEM observation is also insufficient for the quantification of Lemon's connectivity. Due to the limited field of view by SEM, the open channel of the pore can be missed. Lemon's connectivity can be measured by infiltrating the setting polymer in the porous body, as shown in this work. This simple method implies that a pore filled with resin is connected by at least one neighboring pore and eventually from the outside of the porous body. Therefore, the hemiporous scaffold used in this study had the 88% of connectivity exactly defined by Lemon, but the connectivity by Andersson was not confirmed.

According to the result shown in Fig. 8, the efficiency of the cellular infiltration into the scaffold was superior in terms of preloading compared to cellular migration after implantation. The cells suspended in the DMEM should be in favorable condition for migration compared with the cells in the bodily fluid. Eighty-eighty percent of connected pores from the outside, though sufficient coordination among pores was not confirmed, was sufficient for successful cellular migration by preloading. Conclusively, the specimen prepared in this work provided ease of handling along with successful infiltration of cells using the preloading procedure.

The macro porous structure can be embodied using various approaches, such as the use of sacrificial templating materials or by the direct foaming of the ceramic suspensions [32,33].

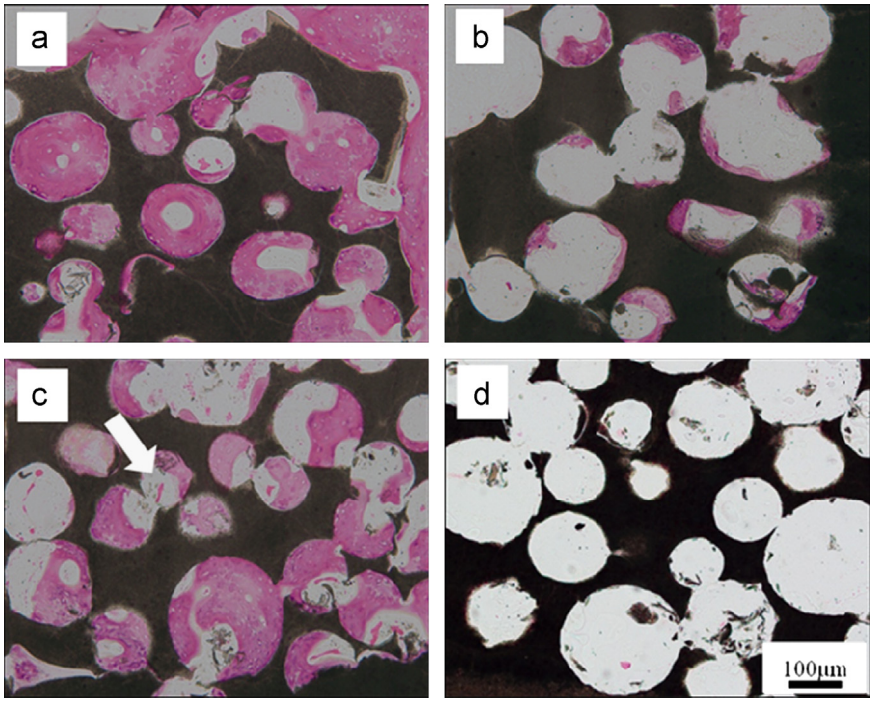

Fig. 8. Photomicrographs showing HE staining results of the specimens after 8 weeks of implantation into distal femur in rabbits (original magnification of × 100). Surface region of hBMSCs-seeded hemiporous HAp scaffold was observed (a) with and (b) without cell loading, respectively. Deep region of hBMSCs-seeded hemiporous HAp scaffold was observed (a) with and (b) without cell loading, respectively. The arrow indicates a tubular newly formed vessel containing red blood cells.

Another technique is to form macroporous ceramic materials from the surfactant or particle stabilized foams or emulsions [34,35]. Recent approach [36] particularly emphasizes the elaborate design of pore structure taking advantage of computer controlled devices. Aim of the approaches should be increase in the coordination among pore as defined by Andersson. However, the result in this work demonstrated that procedure of introducing cells can be more influential compared with the increase in the coordination of pores for successful cellular migration.

In this context, a simple casting approach for scaffold preparation still has merits under the appropriate preloading of cells. In fact, the casting technique can flexibly respond to various demands such as tailoring of pore structure and manipulation of load bearing. In that respect, the present technique showed a simple, economic and versatile approach for designing the scaffold structure without requiring special devices.

5. Conclusion

The aqueous processing of HAp powder successfully produced a hemiporous scaffold that was composed of a porous cell-seeded region and a non-porous load bearing substrate. By pouring the HAp suspension over the stack of porogen placed on the plaster, the specimen with approximately 30 layers of connected pores was prepared. FE-SEM observations demonstrated that hBMSC proliferated and produced extracellular matrices covering the surface of the scaffolds both in the central and in the deep pores at 14 days of the *in vitro* culture. According to the *in vivo* test with rabbits, newly formed bone tissue and tubular newly formed vessels with red blood cells could be verified deep in the hBMSCs-seeded scaffold. The hemiporous HAp scaffold, therefore, provided improved ease of handling along with the interconnected pores sufficient for the migration of hBMSCs by a preloading route.

Acknowledgments

This study was supported by the Korean Ministry of Knowledge Economy (Grant no. 10030019-2010-21) and Basic Science Research Program through the National Research Foundation of Korea (#2011–0026219). Mr. Lee, Min-Chul is acknowledged for his help in mechanical testing.

References

[1] C.G. Finkemeier, Bone-grafting and bone-graft substitutes, Journal of Bone and Joint Surgery-American 84-A (2002) 454–464.
[2] P. Janicki, G. Schmidmaier, What should be the characteristics of the ideal bone graft substitute? Combining scaffolds with growth factors and/or stem cells, Injury 42 (Suppl. 2) (2011) S77–S81.
[3] K. Anselme, Osteoblast adhesion on biomaterials, Biomaterials 21 (2000) 667–681.
[4] R. LeGeros, R. Craig, Strategies to affect bone remodeling: osteointegration, Journal of Bone and Mineral Research 8 (Suppl. 2) (1993) S583–S596.
[5] M. Jarcho, Calcium phosphate ceramics as hard tissue prosthetics, Clinical Orthopaedics and Related Research 157 (1981) 259–278.
[6] K. DeGroot, Bioceramics consisting of calcium phosphate salts, Biomaterials 1 (1980) 47–50.

[7] C. Begley, M. Doherty, R.A.B. Mollan, D.J. Wilson, Comparative study of osteoinductive properties of bioceramics, coral, and processed bone graft substitutes, Biomaterials 16 (1995) 1181–1185.
[8] P. Bianco, M. Riminucci, S. Gronthos, P.G. Robey, Bone marrow stromal stem cells: nature, biology, and potential applications, Stem Cells 19 (2001) 180–192.
[9] H.S. Lee, G.T. Huang, H. Chiang, L.S. Chiou, M.H. Chen, C.H. Hsieh, C.C. Jiang, Multipotential mesenchymal stem cells from femoral bone marrow near the site of osteonecrosis, Stem Cells 21 (2003) 190–199.
[10] M.F. Pittenger, A.M. Mackay, S.C. Beck, R.K. Jaiswal, R. Douglas, J.D. Mosca, M.A. Moorman, D.W. Simonetti, S. Craig, D.R. Marshak, Multilineage potential of adult human mesenchymal stem cells, Science 284 (1999) 143–147.
[11] S.M. Seo, D.M. Kim, T.J. Chung, J.J. Yoo, H.J. Kim, H.J. Chun, J.W. Jang, K.S. Oh, Effect of milling time on the viscosity of hydroxyapatite suspension, Current Applied Physics 12 (2012) S71–S75.
[12] K.S. Oh, F. Caroff, R. Famery, M.F. Sigot-Luizard, P. Boch, Preparation of TCP–TiO_2 biocomposites and study of their compatibility, Journal of the European Ceramic Society 18 (1998) 1931–1937.
[13] J.J. Yoo, W.S. Song, K.H. Koo, K.S. Yoon, H.J. Kim, Osteogenic abilities of bone marrow stromal cells are not defective in patients with osteonecrosis, International Orthopaedics 33 (2009) 867–872.
[14] N. Jaiswal, S.E. Haynesworth, A.I. Caplan, S.P. Bruder, Osteogenic differentiation of purified, culture-expanded human mesenchymal stem cells *in vitro*, Journal of Cellular Biochemistry 64 (1997) 295–312.
[15] K. Donath, G. Breuner, A method for the study of undecalcified bones and teeth with attached soft tissues. The Sage-Schliff (sawing and grinding) technique, Journal of Oral Pathology and Medicine 11 (1982) 318–326.
[16] S.H. Shin, J.J. Yoo, H.N. Kim, H.J. Kim, Enhanced cellular responses of human bone marrow stromal cells cultured on pretreated surface with allogenic platelet-rich plasma Connective Tissue Research 53 (2012) 318–326.
[17] C.B. Chang, J.J. Yoo, W.S. Song, D.J. Kim, K.H. Koo, H.J. Kim, Transfer of metallic debris from the metal surface of an acetabular cup to artificial femoral heads by scraping: comparison between alumina and cobalt-chrome heads, Journal of Biomedical Materials Research Part B Applied Biomaterials 85 (2008) 204–209.
[18] C. Pittet, J. Lemaitre, Mechanical characterization of Brushite cements: a Mohr circles' approach, Journal of Biomedical Materials Research 53 (2000) 769–780.
[19] P.W. Hui, P.C. Leung, A. Sher, Fluid conductance of cancellous bone graft as a predictor for graft–host interface healing, Journal of Biomechanics 29 (1996) 123–132.
[20] K.A. Gross, L.M. Rodriguez-Lorenzo, Biodegradable composite scaffolds with an interconnected spherical network for bone tissue engineering, Biomaterials 25 (2004) 4955–4962.
[21] A.L. Darling, W. Sun, 3D microtomographic characterization of precision extruded poly-epsilon-caprolactone scaffolds, Journal of Biomedical Materials Research Part B-Applied Biomaterials 70B (2004) 311–317.
[22] B. Otsuki, M. Takemoto, S. Fujibayashi, M. Neo, T. Kokubo, T. Nakamura, Pore throat size and connectivity determine bone and tissue ingrowth into porous implants:three-dimensional micro-CT based structural analyses of porous bioactive titanium implants, Biomaterials 27 (2006) 5892–5900.
[23] Y. Kuboki, H. Takita, D. Kobayashi, E. Tsuruga, M. Inoue, M. Murata, N. Nagai, Y. Dohi, H. Ohgushi, BMP-induced osteogenesis on the surface of hydroxyapatite with geometrically feasible and nonfeasible structures: topology of osteogenesis, Journal of Biomedical Materials Research 39 (1998) 190–199.
[24] J.X. Lu, B. Flautre, K. Anselme, P. Hardouin, A. Gallure, M. Descamps, B. Thierry, Role of interconnections in porous bioceramics on bone recolonization *in vitro* and *in vivo*, Journal of Materials Science-Materials in Medicine 10 (1999) 111–120.
[25] G. Lemon, Y. Reinwald, L. White, S. Howdlec, K. Shakesheff, J. King, Interconnectivity analysis of supercritical CO_2-foamed scaffolds, Computer Methods and Programs in Biomedicine 106 (2012) 139–149.
[26] L. Andersson, A. Jones, M. Knackstedt, L. Bergström, Permeability, pore connectivity and critical pore throat control of expandable polymeric sphere templated macroporous alumina, Acta Materialia 59 (2011) 1239–1248.
[27] Q.P. Hou, D.W. Grijpma, J. Feijen, Preparation of interconnected highly porous polymeric structures by a replication and freeze-drying process, Journal of Biomedical Materials Research B 67B (2003) 732–740.
[28] S.J. Gong, H.J. Wang, Q.S. Sun, S.T. Xue, J.Y. Wang, Mechanical properties and *in vitro* biocompatibility of porous zein scaffolds, Biomaterials 27 (2006) 3793–3799.
[29] M.J. Moore, E. Jabbari, E.L. Ritman, L.C. Lu, B.L. Currier, A.J. Windebank, M.J. Yaszemski, Quantitative analysis of interconnectivity of porous biodegradable scaffolds with micro-computed tomography, Journal of Biomedical Materials Research A 71A (2004) 258–267.
[30] Q. Zhang, P.D. Lee, R. Singh, G. Wu, T.C. Lindley, Micro-CT characterization of structural features and deformation behavior of fly ash/aluminum syntactic foam, Acta Materialia 57 (2009) 3003–3011.
[31] P. Spanne, J.F. Thovert, C.J. Jacquin, W.B. Lindquist, K.W. Jones, P. M. Adler, Synchrotron computed microtomography of porous media: topology and transports, Physical Review Letters 73 (1994) 2001–2004.
[32] L. Montanaro, Y. Jorand, G. Fantozzi, A. Negro, Ceramic foams by powder processing, Journal of the European Ceramic Society 18 (1998) 1339–1350.
[33] A.R. Studart, U.T. Gonzenbach, E. Tervoort, L.J. Gauckler, Processing routes to macroporous ceramics: a review, Journal of the American Ceramic Society 89 (2006) 1771–1789.
[34] Z. Du, M.P. Bilbao-Montoya, B.P. Binks, E. Dickinson, R. Ettelaie, B.S. Murray, Outstanding stability of particle-stabilized bubbles, Langmuir 19 (2003) 3106–3108.
[35] D.J. Green, P. Colombo, Cellular ceramics: Intriguing structures, novel properties, and innovative applications, Materials Research Bulletin 28 (2003) 296–300.
[36] F. Fierz, F. Beckmann, M. Huser, S. Irsen, B. Leukers, F. Witte, O. Degistirici, A. Andronache, M. Thie, B. Muller, The morphology of anisotropic 3D-printed hydroxyapatite scaffolds, Biomaterials 29 (2008) 3799–3806.